High resolution 162 MeV pion scattering to 6^- stretched states in ^{26}Mg

B. L. Clausen
Geoscience Research Institute, Loma Linda University, Loma Linda, California 92350
and Physics Department, La Sierra University, Riverside, California 92515

R. J. Peterson, C. Kormanyos, and J. E. Wise
Nuclear Physics Laboratory, University of Colorado, Boulder, Colorado 80309

A. B. Kurepin and Y. K. Gavrilov
Institute for Nuclear Research, 60th October Anniversary Prospect 7A, 117312, Moscow, Russia
(Received 26 April 1993)

Inelastic $\pi^{\pm}$ cross-section measurements at a pion incident energy of 162 MeV were made for 12 previously known 6^- states in ^{26}Mg. The peak resolution was significantly improved over a previous ^{26}Mg(π,π') report describing only two 6^- states. Using both harmonic oscillator and Woods-Saxon wave functions (unbound as necessary), the pion scattering data were combined with electron scattering data to determine the isoscalar magnetic structure coefficients for each state. Although more stretched transitions have been located by pion scattering on ^{26}Mg than in any other nucleus, the total isoscalar strength was only 12% of the extreme single particle sum rule, and only about 1/4 of that predicted by more complete calculations. Discrepancies between the isoscalar strengths for several of these states and those found from a combined electron-proton scattering analysis are pointed out.

PACS number(s): 25.80.Ek

I. INTRODUCTION

One-particle–one-hole stretched excitations, i.e., those formed by coupling the highest-spin orbitals in two successive nuclear shells to the maximum angular momentum, were in the past expected to be relatively simple shell-model states. Because of this, stretched excitations have been studied in a number of different nuclei using many different reactions [1]. One of the most extensively studied nuclei is ^{26}Mg, where the $(f_{7/2}d_{5/2}^{-1})6^-$ transitions have been observed using electron scattering [2, 3], pion scattering [4], proton scattering [5], and the $(\alpha,^3\mathrm{He})$ reaction [6]. Analog 6^- states in ^{26}Al have also been studied by the (p,n) reaction [7], and by nucleon transfer reactions [8–11].

The ^{26}Mg 6^- stretched transitions from the *sd* shell are particularly interesting because of the number of stretched states that have been observed in this non-self-conjugate nucleus. These transitions provide a comparison with the more limited number of 4^- stretched excitations observed in *p*-shell nuclei, but yet are not as complicated as the 8^- stretched states in the open *fp*-shell nuclei for which it is difficult to do shell-model calculations. The only other *sd*-shell nuclei where stretched states have been reported are self-conjugate, in which case any 6^- stretched excitation is expected to be either purely isoscalar or purely isovector. One of each has been observed by pion scattering on ^{24}Mg and ^{28}Si [4, 12], although a second T=1 6^- state has recently been reported for ^{28}Si from electron scattering [13]. A number of supposedly pure isovector 6^- states have been observed in the ^{32}S nucleus [14]. In contrast, coherent mixtures of isoscalar and isovector strengths are allowed between the T=1 states in ^{26}Mg due to its neutron excess. The non-self-conjugate ^{30}Si nucleus is a similar case, but the incomplete electron scattering data for 6^- stretched states have only partially been analyzed [15].

Pion scattering near the $\Delta_{3,3}$ resonance is able to determine the isoscalar component of the transition strength, because it selectively excites isoscalar transitions by a factor of 4–1 over isovector transitions. Using this well-known ratio, the isoscalar strength can be determined in a calibrated, model-independent way based on isovector amplitudes also determined from the well-understood electron scattering reaction where the isovector component is selectively excited and quantitatively reliable. Thus a combined electron-pion analysis is more reliable than other methods for determining isoscalar strength (see Ref. [1] for more details). Both electron and pion scattering excite unnatural parity states by a transverse coupling to the spin.

A previous (150 and 180 MeV) pion scattering experiment with 250–330 keV resolution [4, 16] used a combined electron-pion analysis to determine the isoscalar and isovector strengths for two strong 6^- states observed in ^{26}Mg at 9.18 and 18.05 MeV. In this (162 MeV) pion scattering experiment with a much better resolution of 170 keV, the isoscalar and isovector components have been determined for a total of 12 6^- states known from other reactions. This paper compares the ^{26}Mg structure coefficients from a combined electron-pion analysis to those from a previous electron-proton analysis [5] and discusses the differences.

It has been generally observed that the strength of stretched transitions is significantly less than that expected for a single particle-hole excitation, with the

isoscalar component affected even more strongly than the isovector [1, 17, 18]. In an attempt to explain the lack of experimental strength, various theoretical calculations for *sd*-shell nuclei have included the use of a deformed model [19], a large basis shell-model space [20, 21], and unbound wave functions [3]. The even smaller isoscalar strength than isovector has been attributed to differences in the structure of the two types of transition densities [22, 23]. However, even the most promising calculations overpredict the isoscalar strength in ^{28}Si by 50% and in ^{24}Mg by a factor of 4 [4]. In this paper we compare the magnitudes of the ^{26}Mg structure coefficients with those determined from a simple single particle-hole excitation, as well as from large basis shell-model calculations, and discuss the discrepancies for this important question of nuclear isoscalar magnetism.

II. EXPERIMENTAL DETAILS

This experiment was performed at the Clinton P. Anderson Meson Physics Facility (LAMPF) of the Los Alamos National Laboratory using 162 MeV π^+ and π^-. The target was constructed at the Institute for Nuclear Research in Moscow with an areal density of 70.6 mg/cm^2 and containing 95.5% ^{26}Mg, 2.9% ^{24}Mg, and 1.6% ^{25}Mg. Based on an analysis of the pion scattering spectra, the target also contained about 5% ^{16}O and up to possibly 0.5% calcium or potassium. Inelastic pion scattering data were taken at spectrometer angles of 55°, 75°, and 90° for π^+, and 75° and 90° for π^- using the Energetic Pion Channel and Spectrometer (EPICS) facility, described elsewhere [24]. These angles were expected to be near the maximum of the angular distribution for $M6$ excitations. Spectra with lower statistical accuracy were taken at 30° and 40° to ensure that any angular distribution with a maximum at 75° was not a second maximum of a low multipolarity excitation. Low statistics were also taken at 65°, 80°, and 100° to give a more complete angular distribution. At most angles, and for both π^+ and π^-, data were taken on targets of CH_2 and Mylar to determine energy calibration and cross-section normalization. The resolution was enhanced over that for the previous ^{26}Mg(π,π') 6^- data by the use of, among other things, a thinner vacuum window and a reduced number of chamber planes in the front of the spectrometer [25]. For long runs at back angles the resolution was approximately 170 keV full width at half maximum (FWHM).

Two spectra, corrected for spectrometer acceptance and pion survival, are shown in Fig. 1. Data analysis used the line-shape fitting program ALLFIT [26] with an empirical linear background connecting smooth regions of the spectra and a reference peak shape from an isolated low-lying state. The energy calibration at each angle utilized the prominent states in ^{12}C as well as known, low-lying ^{26}Mg states. The calibration generally found about 99 channels equal to 1 MeV. Excitation energies of the 6^- states determined from pion scattering are listed in Ta-

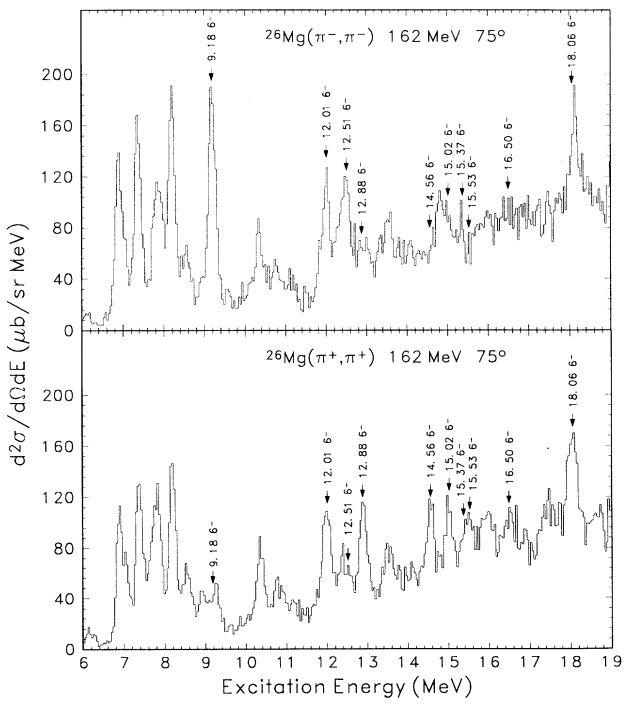

FIG. 1. Spectra from inelastic scattering of 162 MeV π^+ and π^- on ^{26}Mg at a laboratory scattering angle of 75°. The 6^- stretched transitions are labeled. Each energy bin is 40 keV wide.

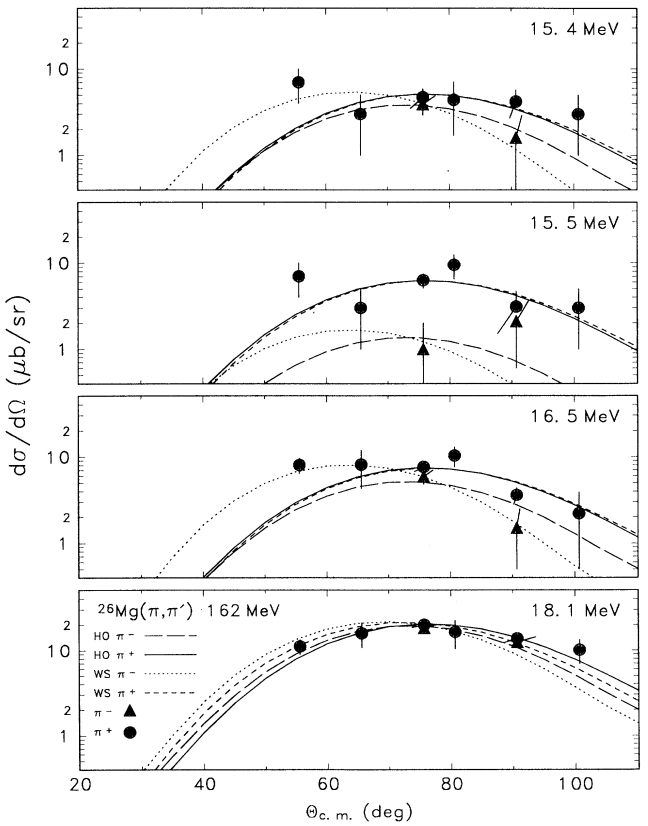

FIG. 2. The $\pi^\pm$ data for ^{26}Mg 6^- states that are predominantly isovector excitations. The DWIA calculations use both HO and WS wave functions.

TABLE I. A comparison of excitation energies for ^{26}Mg 6^- stretched states [and the analogs in ^{26}Al for (p,n)] from several different reactions.

E_x (MeV) (π,π)	E_x (MeV) (e,e')[a]	E_x (MeV) (p,p')[b]	E_x (MeV) ^{26}Mg(p,n)[c]	E_x (MeV) ^{25}Mg$(\alpha,^3$He$)$[d]
	7.54±0.02			
9.18±0.03	9.17±0.01	9.18±0.03	9.3±0.1[e]	9.169±0.005
12.01±0.05		11.98±0.03	12.0±0.1	11.945±0.010
12.51±0.06	12.50±0.04	12.49±0.03	12.5±0.1	12.512±0.010
12.88±0.05	12.88±0.05	12.85±0.03	13.1±0.1	12.865±0.010
	13.00±0.04			12.958±0.010
	13.97±0.03		14.0±0.1	13.958±0.010
14.56±0.05	14.50±0.05	14.50±0.05	14.6±0.1	14.542±0.010
15.02±0.06			15.0±0.1	
15.37±0.11	15.36±0.04	15.36±0.05	15.5±0.1	
15.53±0.09	15.46±0.07	15.46±0.05		
16.50±0.09	16.5	16.50±0.05	16.5±0.1	16.58 ±0.010
18.06±0.04	18.05±0.07	18.05±0.05	18.2±0.1	

[a] Reference [2].
[b] Reference [5].
[c] Reference [7].
[d] Reference [6].
[e] T=0+1.

ble I and compared to those found previously with electron scattering [2, 3], proton scattering [5], the $(\alpha,^3$He) reaction [6], and the (p,n) reaction [7]. The pion excitation energies are equal within uncertainties to those found using the other reactions to ^{26}Mg, and all peaks are narrow relative to our resolution, except for the 16.5 MeV structure.

The 6^- cross sections were normalized to previously known π-^{12}C and π-^{16}O elastic scattering cross sections [27,28]. In an additional check, we found good agreement with previous ^{12}C inelastic scattering cross sections [29] and with a $\theta_{\rm lab}$=75° $\pi^+ + p$ center-of-mass cross section of 8.48 mb/sr [30]. The normalization factor for the spectrometer was smaller by a factor of 0.8 for π^- than for π^+ cross sections, similar to results found previously [24, 18]. The total systematic error was about 8%, with 6%

TABLE II. Center-of-mass pion scattering cross sections for states observed in ^{26}Mg. Scattering angles are given in the center-of-mass frame. The listed uncertainties include both statistical and systematic errors. An asterisk indicates where no peak was observed for an excited state at a particular scattering angle.

E_x (MeV)	J^π	$\sigma^\pm$ (μb/sr)			
		75.7° π^-	90.7° π^-	30.4° π^+	40.5° π^+
8.91		4.5±0.8	1.4±0.7	201±13.0	110±7.0
9.18	6^-	33.0±3.0	25.8±3.2	*	*
9.28		*	*	58.0±7.2	31.3±4.4
10.34		14.1±1.3	18.4±1.8	122±9.0	121±8.0
10.74		7.8±0.9	1.4±1.1	66.6±7.7	60.9±6.4
11.86		4.5±1.3	5.8±1.5	121±33.0	61.8±6.5
12.01	6^-	14.5±1.7	5.7±1.6	*	*
12.27		8.5±1.3	4.1±1.1	38.9±7.8	37.0±4.3
12.51	6^-	14.3±1.6	9.8±1.3	< 15	< 15
12.88	6^-	4.1±1.1	2.5±1.2	*	< 5
13.01	6^-	3.5±1.1	2.6±1.7	< 15	*
13.52		7.6±1.2	3.8±0.9	44.3±7.6	44.7±4.7
13.97	6^-	< 2	< 1	*	*
14.56	6^-	1.1±0.8	< 1	< 10	< 20
15.02	6^-	5.3±1.2	3.9±1.2	*	*
15.37	6^-	3.9±1.0	1.6±1.3	< 20	< 30
15.53	6^-	< 2	2.1±1.5	< 10	< 20
16.50	6^-	5.9±1.1	1.5±1.0	*	*
18.06	6^-	18.3±1.8	12.5±1.8	< 30	< 10

TABLE III. Center-of-mass pion scattering cross sections for states observed in ^{26}Mg. Scattering angles are given in the center-of-mass frame. The listed uncertainties include both statistical and systematic errors. An asterisk indicates where no peak was observed for an excited state at a particular scattering angle.

E_x (MeV)	J^π	$\sigma^\pm$ (μb/sr)					
		55.6° π^+	65.6° π^+	75.7° π^+	80.7° π^+	90.7° π^+	100.7° π^+
8.91		25.1±2.3	12.6±3.1	6.6±0.6	3.6±1.5	7.0±0.8	4.5±1.5
9.18	6⁻	*	<5	3.0±1.1	*	1.5±1.3	<4
9.28		33.5±3.6	15.3±5.2	4.2±1.0	5.4±2.0	9.4±1.4	7.6±2.3
10.34		86.3±6.4	30.6±5.0	13.1±1.0	19.4±2.9	27.2±2.3	34.6±4.5
10.74		15.7±1.7	4.5±2.5	5.7±0.8	6.5±1.8	4.2±0.6	4.5±1.5
11.86		16.2±2.0	*	3.3±1.0	1.7±1.5	9.0±1.1	7.0±2.3
12.01	6⁻	2.0±1.8	14.4±6.0	14.8±1.3	14.9±3.0	8.9±1.3	2.8±2.4
12.27		14.7±2.2	6.1±3.1	*	6.2±2.3	3.4±0.9	2.6±1.5
12.51	6⁻	*	*	2.0±1.3	4.7±2.1	4.6±1.6	*
12.88	6⁻	13.0±2.1	12.0±5.0	14.6±1.6	15.4±5.8	15.4±2.5	12.6±9.1
13.01	6⁻	2.7±2.1	<3	<2	< 5	<2	<2
13.52		13.8±1.9	7.6±3.1	7.0±0.8	7.2±4.9	5.2±1.3	6.5±2.1
13.97	6⁻	<5	<2	< 2	2.0±1.8	1.7±0.6	2.0±1.5
14.56	6⁻	10.0±2.2	18.6±4.3	11.9±1.0	11.6±2.6	8.6±1.0	5.3±1.8
15.02	6⁻	6.7±1.4	8.4±3.7	10.5±1.0	10.6±2.8	10.1±1.1	7.8±2.5
15.37	6⁻	7.0±3.0	3.0±2.0	4.7±1.2	4.4±2.7	4.2±1.5	3.0±2.0
15.53	6⁻	7.0±3.0	3.±2.0	6.3±1.2	9.5±3.0	3.1±1.6	3.0±2.0
16.50	6⁻	8.0±1.6	8.1±3.8	7.6±0.9	10.3±2.7	3.6±0.8	2.2±1.7
18.06	6⁻	11.2±2.2	15.9±5.1	20.0±1.5	16.5±6.1	13.8±1.4	10.1±3.2

due to uncertainties in the absolute normalization. The pion scattering cross sections are listed in Tables II and III and plotted in Figs. 2–5 along with their errors that include both statistical and systematic uncertainties.

III. ANALYSIS

A. DWIA calculations

The analysis described here follows closely that reported in Refs. [3] and [18], and more details can be found there. The distorted-wave impulse-approximation (DWIA) calculations used the codes ALLWRLD [31] and MSUDWPI [32] with the spin-orbit force and optical potential parameters similar to that reported previously, and a charge radius of 3.06 fm determined from electron scattering [33]. The ground-state density distribution parameters used for both protons and neutrons in these two codes were assumed to have a Woods-Saxon form $\rho(r) \propto [1 + e^{(r-c)/a}]^{-1}$ with radius c=2.88 fm and diffuseness a=0.52 fm, taken from a previous pion scattering analysis [16].

The two sets of transition densities input to ALLWRLD used pion scattering parameters fixed at the values found to fit best the stretched state

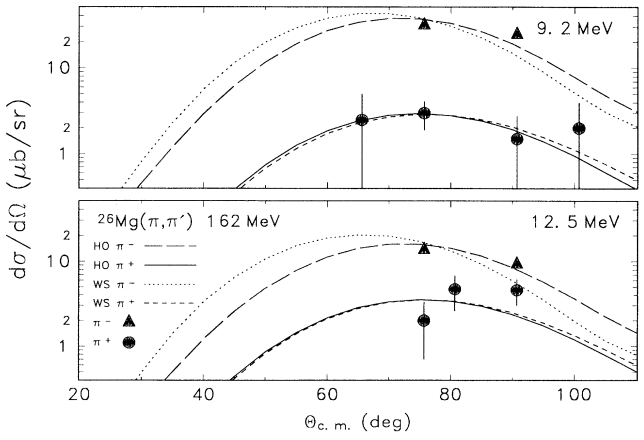

FIG. 3. The $\pi^\pm$ data for ^{26}Mg 6⁻ states that are predominantly neutron excitations. The DWIA calculations use both HO and WS wave functions.

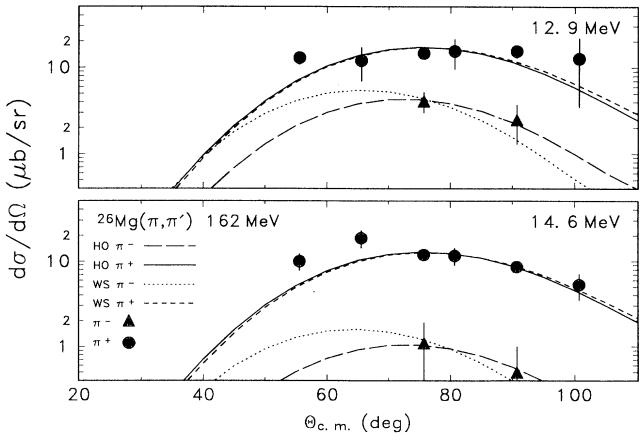

FIG. 4. The $\pi^\pm$ data for ^{26}Mg 6⁻ states that are predominantly proton excitations. The DWIA calculations use both HO and WS wave functions.

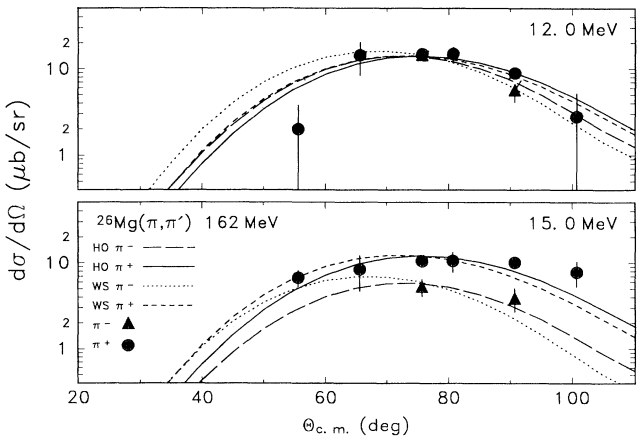

FIG. 5. The $\pi^{\pm}$ data for ^{26}Mg 6^- states that are predominantly isoscalar excitations. The DWIA calculations use both HO and WS wave functions.

electron scattering data. The set with simple harmonic oscillator (HO) single-nucleon wave functions used b=1.77±0.07 fm. The set with Woods-Saxon (WS) wave functions (which are especially important for unbound states) used r_0=1.30±0.06 fm and diffuseness and spin-orbit parameters of a=0.65 fm and λ=25, respectively. The WS proton and neutron wave functions were calculated based on the respective separation energies. The proton (neutron) binding energy used for a given excited state was its excitation energy minus the proton (neutron) separation energy of 14.14 (11.09) MeV. The $5/2^+$ ground state in mass 25 was taken as the hole for the stretched excitation, except for the 18.1 MeV T=2 state, where the lowest T=3/2 state in ^{25}Mg was used for the neutron-hole state. Its excitation energy of 7.78 MeV was subtracted in addition to the 11.09 MeV neutron separation energy to arrive at the neutron binding energy.

The WS wave functions calculated with DWUCK4 [34] for both electron and pion scattering used a nonlocal parameter (PNLOC) of zero. In Ref. [3], a value of PNLOC of 0.85 was used, in which case r_0=1.24±0.07 fm was needed for a best fit to the stretched state electron scattering data. With PNLOC of 0, the WS $(M_1^e)^2$ listed in Table IV are from 4% to 20% less than those listed in the previous work, allowing an estimate of the model-dependent uncertainty in our results.

B. Structure coefficient calculations

The differential cross section for pion scattering to stretched magnetic transitions can be written schematically as

$$\sigma^{\pm} = N\, f_{\text{c.m.}}^2\, (M_1^{\pm})^2 \left[\frac{M_0^{\pm}}{M_1^{\pm}} Z_0 + Z_1\right]^2 , \qquad (1)$$

where N is an empirical normalization of the pion calculated cross sections (assumed here to be equal for π^+ and π^-) to known isovector electron scattering strengths, $M_\tau^{\pm}$ are matrix elements calculated in the DWIA, and Z_τ are spectroscopic coefficients for a pure isoscalar (τ=0) or isovector (τ=1) single particle-hole $(f_{7/2}d_{5/2}^{-1})6^-$ transition. For incident pion energies near the $\Delta_{3,3}$ resonance, $M_0^{\pm}/M_1^{\pm} \approx \mp 2$ for $\pi^{\pm}$ scattering. The standard center-of-mass correction was made by reducing the HO b or the WS r_0 derived from electron scattering by $[(A-1)/A]^{1/2}$,

TABLE IV. Values used to calculate the structure coefficients in ^{26}Mg. The experimental cross sections for pion scattering at the top of the angular distribution are from a least-squares fit to the data. (The listed values are an average between the peak of the fits for HO and those for WS, which for π^- could be quite different.) The theoretical DWIA pion cross sections, $(M_1^\pi)^2$, at the peak of the angular distribution were calculated using ALLWRLD and MSUDWPI. The experimental form factors, F^2, for electron scattering from Refs. [2] and [3] were determined in a similar fashion and are also listed. The theoretical electron cross section, $(M_1^e)^2$, at the peak of the angular distribution, is 48.2×10^{-5} for HO wave functions and is listed for the WS wave functions. None of the calculations included meson exchange current (MEC) effects.

			HO		WS			WS
E_x (MeV)	σ^- (μb/sr)	σ^+ (μb/sr)	$(M_1^-)^2$ (μb/sr)	$(M_1^+)^2$ (μb/sr)	$(M_1^-)^2$ (μb/sr)	$(M_1^+)^2$ (μb/sr)	10^5F^2	$10^5(M_1^e)^2$
7.5							0.1	
9.2	40.0±9.0	< 3	88.1	83.9	104.5	71.8	1.5±0.1	45.6
12.0	15.0±2.0	14.1±1.5	85.0	80.8	93.5	73.6		
12.5	18.0±4.0	< 5	84.3	80.1	93.3	73.8	2.0±0.1	40.3
12.9	4.9±1.1	17.1±2.2	83.9	79.7	92.3	74.0	0.9±0.1	39.6
13.0	4.0±1.0	< 2	83.8	79.6	95.0	73.3	0.5±0.1	39.7
14.0	< 2	< 3	82.7	78.5	93.6	73.2	0.7±0.1	37.9
14.6	< 2	12.7±1.0	82.2	78.0	97.4	71.8	1.1±0.1	37.3
15.0	6.4±1.5	12.2±1.2	81.5	77.4	102.0	66.1		
15.4	4.6±1.2	5.1±0.8	81.2	77.0	108.2	68.2	1.2±0.1	36.7
15.5	< 3	6.2±0.9	81.1	76.9	112.3	67.0	2.2±0.2	36.9
16.5	6.5±2.0	7.4±1.1	80.0	75.7	126.4	61.3	2.6±0.4	36.0
18.1	20.0±3.0	20.8±1.4	78.3	74.1	90.4	61.6	7.1±0.7	37.2

before using it for the (π,π') DWIA calculations. The final theoretical cross sections were then increased by $f^2_{\text{c.m.}} = [A/(A-1)]^L$, equal to 1.22 for ^{26}Mg, L=5 6^- transitions. The simplifying characteristics of stretched excitations which justify the form of Eq. (1) have been discussed elsewhere [1]. A similar formulation was used for analysis of the proton scattering on ^{26}Mg [5].

A similar equation can be written for electron scattering in order to compare pion and electron scattering data:

$$F^2 = (M^e_1)^2 \left[\frac{M^e_0}{M^e_1} Z_0 + Z_1\right]^2 , \qquad (2)$$

where nucleon finite size and center-of-mass factors are contained in the isoscalar and isovector electromagnetic matrix elements M^e_0 and M^e_1. Distorted-wave Born approximation effects are included in the standard q_{eff} approximation.

The magnitude of the calculated DWIA pion angular distribution was varied to fit the data for each ^{26}Mg 6^- state until a best χ^2 fit was obtained as shown in Figs. 2–5. The resulting $\sigma^{\pm}$ at the peak of the form factor as used in Eq. (1) are listed in Table IV. [For electron scattering the F^2 used in Eq. (2) were determined by a similar procedure and are also listed in Table IV.] The π^+ data are fit equally well with HO or WS wave functions, but the π^- data are fit somewhat better using HO than using WS wave functions in several cases. The pion cross-section data unambiguously determine the 6^- multipolarity for those states having a strong π^+ component, in which case there is good data from 55° to 100°, and marginal data at 30° and 40°. For the two important states that do not have a strong π^+ component (at 9.2 and 12.5 MeV and shown in Fig. 3), the two strong π^- data points are insufficient to unambiguously determine the multipolarity. Instead, we base our 6^- assignment on the fact that the excitation energies determined for these two prominent π^- peaks are the same as for two corresponding prominent 6^- states in the other reactions listed in Table I. In addition, the π^- data for these two states are not inconsistent with a 6^- multipolarity assignment. In some cases the agreement between computed and measured shapes is not good, perhaps indicating something other than a simple stretched 6^- state. If so, our extracted strengths are an overestimate, and the true fractions of the sum rules will be lower.

The cross sections were calculated by ALLWRLD and MSUDWPI using both HO and WS wave functions, and the $(M^e_1)^2$ were calculated with an electron scattering code in the q_{eff} approximation. Results are given in Table IV. The M^π_0/M^π_1 ratio used in Eq. (1) for 162 MeV pion scattering was determined from ALLWRLD and MSUDWPI to be 1.93 for HO wave functions and varied from 1.7 to 2.1 for WS wave functions, depending upon the excitation energy and pion charge. The M^e_0/M^e_1 ratio used in Eq. (2) for electron scattering was −0.187 for HO wave functions and varied from −0.15 to −0.27 for WS wave functions, depending upon the excitation or binding energy.

Using these known values for the cross sections and matrix elements, Eqs. (1) and (2) were solved simultaneously for Z_0, Z_1, and N. Two different computational methods were used. The ratio method was used for all states where the electron and both pion scattering cross sections were known. In this method the structure coefficients are independent of the theoretical pion scattering calculations and depend only on the M^π_0/M^π_1 ratio near $\Delta_{3,3}$ resonance energies. Once the structure coefficients were calculated, it was possible to determine the normalization factor necessary to arrive at agreement with theoretical pion scattering calculations. These factors and their uncertainties are shown in Fig. 6. As can be seen, the normalization varies considerably, since all except the 18.1 MeV state had poor data for at least one of the three reactions. Because of this, the absolute method was used for all quoted results. This method used two of the three cross sections, plus an average normalization determined from the previous method. The average normalization of N_{HO}=1.4±0.1 and N_{WS}=1.2±0.1 was based mainly on the purely isovector 18.1 MeV T=2 state. That these values are near unity is a sign that our DWIA calculations are nearly absolutely correct.

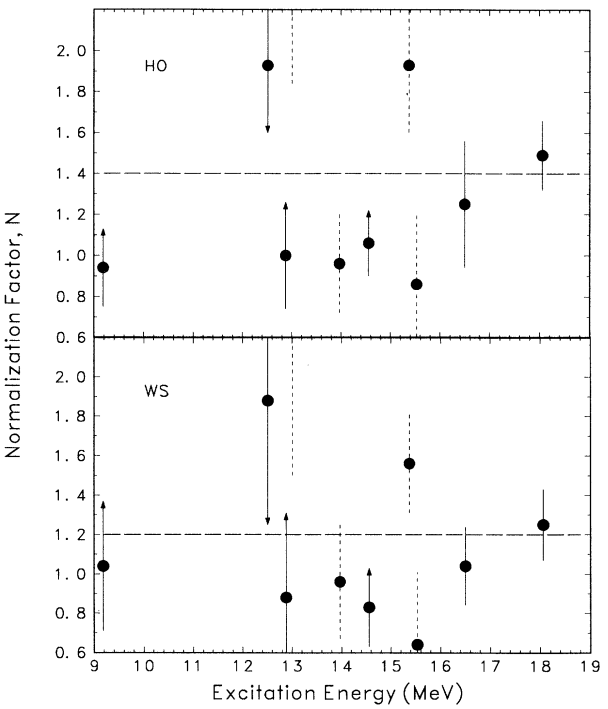

FIG. 6. Normalization factors determined for each state from both the HO and the WS analyses. Dashed lines are for questionable factors from states with small cross sections. Arrows are included for states where either π^+ or π^- was small and a limit can be determined for the factor from only one direction. The horizontal line indicates the average normalization used for calculating all Z coefficients, where N=1 would correspond to an ideal description of the reaction by the DWIA model.

C. Structure coefficients

The Z coefficients calculated with the above method using both HO and WS wave functions are tabulated in

TABLE V. A tabulation of Z coefficients for ^{26}Mg 6^- stretched states extracted from a combined analysis of electron and pion scattering data. Both HO and WS wave functions were used, and no MEC effects have been included. The Z_1 coefficients have arbitrarily been chosen to be the positive solution. In all cases, the Z coefficients were determined by the absolute method using an average normalization of $N_{\rm HO}$=1.4 and $N_{\rm WS}$=1.2.

E_x	HO		WS	
(MeV)	Z_0	Z_1	Z_0	Z_1
9.2	0.15±0.03	0.21±0.01	0.18±0.04	0.22±0.01
12.0	0.16±0.01	0.00±0.01	0.19±0.01	0.00±0.01
12.5	0.06±0.01	0.22±0.01	0.08±0.03	0.24±0.01
12.9	-0.13±0.02	0.11±0.01	-0.15±0.02	0.11±0.01
13.0	0.03±0.03	0.11±0.01	0.04±0.01	0.12±0.01
14.0	0.00±0.01	0.12±0.01	0.00±0.01	0.13±0.01
14.6	-0.09±0.01	0.13±0.01	-0.10±0.01	0.14±0.01
15.0	-0.13±0.01	0.05±0.01	-0.15±0.01	0.05±0.02
15.4	-0.02±0.02	0.15±0.01	0.00±0.01	0.18±0.01
15.5	0.00±0.01	0.21±0.01	0.00±0.01	0.25±0.01
16.5	-0.01±0.01	0.23±0.02	-0.03±0.01	0.26±0.02
18.1	0	0.38±0.02	0	0.44±0.02
$\sum Z_\tau^2$=	0.10±0.01	0.41±0.02	0.13±0.02	0.53±0.02

Table V. The use of WS wave functions in the analysis increased the $\sum Z_\tau^2$ by about a factor of 1.3 over that determined for HO wave functions. If isovector meson exchange current (MEC) contributions had been included in the electron scattering calculations [35], the theoretical cross sections would be 11%–15% larger, thus reducing the value of the Z^2 coefficients by the same amount.

In all calculations, the Z_1 coefficient is mainly determined by the electron scattering data and is inversely related to the theoretical electron scattering matrix elements. The magnitude of Z_0, on the other hand, is determined relative to Z_1 from the π^+/π^- cross-section ratio near resonance. Thus Z_0 is not proportional to the pion scattering matrix element; only the normalization N is. Similarly, the use of WS wave functions in the pion scattering analysis has little direct effect on the Z_0 structure coefficients; however, changing the value of the Z_1 coefficient changes the Z_0 coefficient by the same fraction due to a corresponding inverse change in the value of the normalization factor N.

The sums of the squares of the Z coefficients derived using HO wave functions are tabulated in Table VI. These experimental structure coefficients can in the first approximation be compared to the extreme single-particle-hole-model (ESPHM) sum rules given in Ref. [36]. The total structure coefficients for ^{26}Mg should add to $\sum Z_0^2 = \sum Z_1^2 = 5/6$. The isovector component can be divided into $\sum Z_1^2 = 1/2$ for the T=1 states

TABLE VI. Listed here are the sums of the experimental Z coefficients derived from a combined electron-pion analysis for the 6^- states in ^{26}Mg. They are compared to results from a similar analysis for ^{24}Mg and ^{28}Si [21]. Harmonic oscillator wave functions were used with no MEC effects included. The theoretical Z coefficients are from the extreme single-particle-hole-model (ESPHM) sum rules of Ref. [36] and from the large basis shell-model (LBSM) calculations of Refs. [21] and [37]. The ratio between experiment and theory is defined as $S_\tau^2 = \sum(Z_\tau^2)_{\rm expt} / \sum(Z_\tau^2)_{\rm th}$.

	τ	$\sum(Z_\tau^2)_{\rm expt}$	Z_0^2/Z_1^2	$\sum(Z_\tau^2)_{\rm th}$		S_τ^2	
				ESPHM	LBSM	ESPHM	LBSM
^{24}Mg			0.26				
	0	0.05		2/3	0.20	0.07	0.25
	1	0.19		2/3	0.32	0.29	0.59
^{26}Mg			0.23				
	0	0.10		5/6	0.44	0.12	0.23
	1	0.41		5/6	0.52	0.49	0.79
	T=1	0.27		1/2	0.32	0.54	0.84
	T=2	0.14		1/3	0.20	0.43	0.72
^{28}Si			0.45				
	0	0.13		1	0.20	0.13	0.65
	1	0.29		1	0.37	0.29	0.78

and $\sum Z_1^2 = 1/3$ for the T=2 states. In a more complete analysis the experimental structure coefficients can be compared to large basis shell-model (LBSM) calculations [37, 21]. Both of these theoretical results are given in Table VI, along with the experiment-to-theory ratio $S_\tau^2 = \sum(Z_\tau^2)_{\rm expt}/\sum(Z_\tau^2)_{\rm th}$.

The total ESPHM strength for ^{26}Mg is significantly less than that predicted by the sum rule, with the isoscalar strength of 12% significantly smaller than the isovector strength of 49%. Even when compared to LBSM calculations, the experimental isoscalar strength is only 1/4 that expected. The fraction of isoscalar strength observed for ^{26}Mg is comparable to that for ^{24}Mg, but significantly less than the 65% observed for ^{28}Si when compared to LBSM calculations, whereas the fraction of LBSM isovector strength of greater than 1/2 is not significantly different between the three nuclei.

IV. DISCUSSION

It is particularly useful to have data now for a nucleus with a large number of different stretched states observed in a wide variety of reactions. Each state will be discussed and the results from pion and proton scattering will be compared, with the results summarized in Table VII.

A. Predominantly isovector excitations

The 7.5, 13.0, and 14.0 MeV transitions were weakly observed in electron scattering. The 7.54 MeV state has only been observed in electron scattering, and there it was a factor of 3 weaker than the next strongest state. The form factor shape was poorly defined, and a 6^- assignment to it was made with very little confidence [2]. We suggest that the 7.54 MeV state is not a 6^- transition and do not include it in our analysis. The 13.0 and 14.0 MeV transitions were not observed by pion scattering, except for a possible weak π^- peak at 13.0 MeV, and therefore must be predominantly isovector. These two states were not observed by proton scattering [5]; however, the 14.0 MeV state was observed with the (p,n) reaction [7], and both the 13.0 and 14.0 MeV states were observed with the high resolution $(\alpha,^3\mathrm{He})$ reaction [6].

The 15.4 and 15.5 MeV states were strongly excited in electron scattering, and the (p,n) reaction excited a state at 15.5 MeV but was unable to resolve two states. There was no evidence in the $(\alpha,^3\mathrm{He})$ neutron transfer reaction for population of either state [6]. From proton scattering the 15.4 MeV state was determined to be mainly a neutron excitation, and the 15.5 MeV state appeared to favor a lower multipolarity assignment [5]. From the pion data the two states were weak and poorly resolved and excited slightly more strongly by π^+ than π^-. Based on pion scattering these two states have little or no isoscalar component.

The 16.5 MeV complex was observed in all of the reactions referred to here, with a particularly strong excitation for electron scattering. No combination of structure coefficients was able to fit both the electron and proton scattering data, but the weakness of the state in (p,p') re-

TABLE VII. Structure coefficients are listed for the ^{26}Mg 6^- transitions derived from our combined electron-pion analysis, where HO wave functions were used and no MEC effects were included. For comparison, coefficients from a combined electron-proton analysis [5] are listed, with alternate sets of coefficients for three states included in brackets. We relate the neutron and proton structure coefficients to the isoscalar and isovector structure coefficients by the convention $Z_n = (Z_0 + Z_1)/\sqrt{2}$ and $Z_p = (Z_0 - Z_1)/\sqrt{2}$. The coefficient for the dominant type of excitation (isoscalar, isovector, neutron, or proton) for each state is underlined.

E_x	(e,e')+(π,π')				(e,e')+(p,p')			
(MeV)	Z_0	Z_1	Z_n	Z_p	Z_0	Z_1	Z_n	Z_p
9.2	0.15	0.21	<u>0.25</u>	-0.04	-0.14	0.15	0.01	<u>-0.20</u>
					[0.23	0.21	<u>0.31</u>	0.02]
12.0	<u>0.16</u>	0	0.11	0.12	<u>0.22</u>	0.04	0.18	0.13
12.5	0.06	<u>0.22</u>	0.20	-0.11	0.23	0.23	<u>0.33</u>	0
					[-0.14	0.17	0.02	<u>-0.22</u>]
12.9	-0.13	0.11	-0.01	<u>-0.17</u>	0.26	0.17	<u>0.30</u>	0.06
13.0	0.03	<u>0.11</u>	0.10	-0.05				
14.0	0	<u>0.12</u>	0.09	-0.09				
14.6	-0.09	0.13	0.03	<u>-0.16</u>	0.16	0.17	<u>0.23</u>	-0.01
					[-0.04	<u>0.16</u>	0.08	-0.14]
15.0	<u>-0.13</u>	0.05	-0.06	-0.13				
15.4	-0.02	<u>0.15</u>	0.09	-0.12	0.19	0.18	<u>0.26</u>	0.00
15.5	0	<u>0.21</u>	0.14	-0.15				
16.5	-0.01	<u>0.23</u>	0.16	-0.17	a	a		
18.1	0	<u>0.38</u>	0.27	-0.27		<u>0.35</u>	0.25	-0.25
$\sum Z_\tau^2$=	0.10	0.41			0.25	0.29		

[a] $|Z_0| < 0.1$ and $|Z_1| < 0.15$.

quired $|Z_0| < 0.1$ and $|Z_1| < 0.15$ [5]. However, the combined electron-pion analysis determined $Z_1 = 0.23 \pm 0.02$ for the complex. The proton scattering spectrum finds a single peak at this excitation.

The ^{26}Mg analog of the T=2 ^{26}Na ground state is expected to have an excitation energy of 12.6 MeV [2]. States in ^{26}Mg which have less than 12.6 MeV excitation are therefore expected to have isospin T=1, while states with more than 12.6 MeV excitation are candidates for an isospin assignment of either T=1 or T=2. The 13.0, 14.0, 15.4, 15.5, and 16.5 MeV states are all (within uncertainties) purely isovector, and thus candidates for a T=2 assignment.

The 18.1 MeV T=2 state is the strongest 6^- excitation in electron scattering and is a dominant excitation in the pion and proton scattering spectra. It is the strongest $T \neq 0$ 6^- excitation in the (p,n) reaction, although a stronger T=0 excitation was observed at 6.9 MeV in ^{26}Al. As expected for a T=2 excitation, this state in ^{26}Mg was not observed with the $(\alpha,^3\mathrm{He})$ reaction. For pion scattering, it was mainly this strong purely isovector state that was used to normalize the DWIA theoretical calculations to experiment. The N_{HO}=1.4±0.1 determined from this analysis was larger than, but equal within uncertainties, the N_{HO}=1.25±0.14 determined for the previous 150 and 180 MeV pion scattering data [4].

B. Predominantly neutron and proton excitations

The 12.5 MeV state is a strong excitation in all the reactions referred to here. With pion scattering, it is strong in the π^- spectrum, but weak and difficult to separate from a doublet in the π^+ spectrum. This pionic signature agrees with the conclusion from proton scattering that it is predominantly a neutron transition. However, if the normalization from the 18.1 MeV state is used in conjunction with the electron and π^- cross sections, the isovector component appears to be much stronger than the isoscalar.

The 9.2, 12.9, and 14.6 MeV states have been observed in all the reactions referred to here. The 9.2 MeV state, the lowest 6^- transition, is strong in the π^- spectra but weak in the π^+ spectra, whereas the 12.9 and 14.6 MeV states are strong excitations in the π^+ spectra, but weak for π^-. The combined electron-pion analysis for these states results in structure coefficients corresponding to predominantly neutron, proton, and proton transitions, respectively. This determination is in agreement with the spectroscopic factors determined for the neutron transfer $(\alpha,^3\mathrm{He})$ reaction, where the 9.2 MeV state is excited by a factor of 10 more strongly than the 12.9 and 14.6 MeV states. With the (p,n) reaction, the 9.2 MeV state in ^{26}Al is excited at least twice as strongly as the other two states. In contrast, the previous combined electron-proton analysis for these states shown in Table VII resulted in structure coefficients corresponding to predominantly proton, neutron, and neutron transitions, respectively [5]. The electron-proton analysis provided a second poorer choice of structure coefficients for the 14.6 (their 14.50) MeV state, giving a predominantly isovector excitation. This second choice is in better agreement with the pion data, and the proton data did not unambiguously distinguish between the two solutions. For the 9.18 MeV state, the discrepancy between proton data and the previous 150 and 180 MeV pion scattering data has been discussed at length [4]. The analysis done here using higher resolution 162 MeV pion scattering data arrives at the same structure coefficients within uncertainties and confirms that discussion.

C. Predominantly isoscalar excitations

Nine additional states between 8 and 14 MeV excitation were analyzed in a search for other possible 6^- transitions. One would expect any such excitation to be predominantly isoscalar, since none of these states was determined to be a 6^- transition from electron scattering. The (π,π') cross sections are listed in Tables II and III. Seven of the states, with excitation energies of 8.91±0.04, 9.28±0.04, 10.34±0.02, 10.74±0.05, 11.86±0.10, 12.27±0.06, and 13.52±0.05 MeV, have experimental angular distributions at small angles incompatible with a 6^- assignment. Several of these states were possibly observed in electron scattering and assigned a 4^- multipolarity [2]. The two other states at 12.01 and 15.02 MeV were not observed at the small scattering angles in this experiment, making a 6^- multipole assignment reasonable.

The 12.0 MeV state has also been observed with proton scattering and the (p,n) and $(\alpha,^3\mathrm{He})$ reactions. We agree with the conclusion from proton scattering that it is predominantly an isoscalar transition (see Table VII), and then question why it was so strongly excited by the (p,n) reaction. The 15.0 MeV state has previously been reported only with the (p,n) reaction, and there as part of a complex of four "states." A distinct state is seen at about 15 MeV in the proton scattering spectra, and possible weak states are seen at that energy in the electron scattering and $(\alpha,^3\mathrm{He})$ spectra; however, none actually report a state at that energy. We find from our combined electron-pion analysis that this state is predominantly isoscalar, but includes a small isovector component.

V. CONCLUSIONS

This ^{26}Mg pion scattering experiment found more stretched transitions than any previous pion scattering experiment, but even so the isoscalar strength was found to be significantly smaller than even the most complete theoretical calculations. However, it should be noticed in Table VI that as the *sd* shell is being filled from ^{24}Mg to ^{28}Si, the isoscalar strength does increase, with the rate of increase being somewhat faster than that theoretically predicted. For the isovector strength determined mainly from electron scattering, a single particle-hole model predicts an increase in the strength to a maximum for ^{28}Si. In contrast, large basis shell-model calculations predict a maximum isovector strength for ^{26}Mg in agreement with experiment.

There appear to be several points of disagreement between this electron-pion analysis and a previous electron-proton analysis [5] as displayed in Table VII. The pri-

mary disagreement has to do with the determination of proton and neutron excitations. By comparing the π^+ and π^- spectra shown in Fig. 1, it is obvious that the 9.2 MeV state is primarily a neutron excitation and the 12.9 and 14.6 MeV states are primarily proton excitations. This is opposite to the determination from a combined analysis of electron and proton scattering data, where the preferred structure coefficients suggest that the 9.2 MeV state is a proton excitation and the 12.9 and 14.6 MeV states are neutron excitations. Two other disagreements between the methods have to do with the magnitude of several structure coefficients. The isoscalar component determined for the 12.5 and 15.4 MeV states is much smaller from the electron-pion analysis than the electron-proton analysis [3]. A much smaller Z_1 coefficient is needed for the 16.5 MeV state based on the electron-proton analysis than that based on an electron-pion analysis.

The disagreement with the proton data is disturbing and has yet to be resolved. The proton analysis for ^{26}Mg [5] used a chain of ratios of three reactions on two targets to infer the isoscalar 6^- strengths, in contrast to the very direct comparison of π^- and π^+ data, with the DWIA calculations renormalized by comparison to electron scattering. For the 9.18 MeV state, the problem with labeling it a proton excitation was already recognized in the proton scattering paper [5]. The general analysis done in that paper recognized that the phases between the isoscalar and isovector scattering amplitudes used in the DWIA proton scattering calculation were questionable. If the phase between M_0^p and M_1^p were reflected about 90°, the proton and neutron states would be interchanged. The disagreements show that the isoscalar component of stretched transitions cannot be confidently determined using only proton scattering.

The spin excitation by zero-spin pions must be transverse (of the form $\sigma \times q$), while the (p,p') reaction can also excite spin transitions by the longitudinal $(\sigma \cdot q)$ form. If the difference between proton and pion results is due to this cause, an interesting new spectroscopic feature will have been revealed. This suggestion of quenched spin transverse and enhanced spin longitudinal cross sections for stretched states has been made by Cohen [38]. Petrovich, Carr, and McManus [39] show this effect to be due to contributions beyond the $1\hbar\omega$ model space considered most simply for stretched states. It would be valuable to compute the ^{26}Mg 6^- proton scattering cross sections in a standard DWBA context using the structure coefficients obtained from pion scattering, using HO wave functions in common. With so many 6^- transitions uniquely available for this system, such a comparison should yield systematic insight into the apparent discrepancy between results of the direct pion analysis and the chain of logic used for the proton analysis.

ACKNOWLEDGMENTS

We wish to thank Travis Johnson for assistance in the data analysis. This work was supported in part by the National Science Foundation and the U.S. Department of Energy, including support through the Association of Western Universities.

[1] R. A. Lindgren and F. Petrovich, in *Spin Excitations in Nuclei*, edited by F. Petrovich *et al.* (Plenum, New York, 1984), p. 323; R. A. Lindgren, J. Phys. (Paris) Colloq. **45**, C4-433 (1984).
[2] M. A. Plum, Ph.D. thesis, University of Massachusetts, 1985.
[3] B. L. Clausen, R. J. Peterson, and R. A. Lindgren, Phys. Rev. C **38**, 589 (1988).
[4] R. A. Lindgren *et al.*, Phys. Rev. C **44**, 2413 (1991).
[5] R. E. Segel *et al.*, Phys. Rev. C **39**, 749 (1989).
[6] J. J. Kraushaar, M. Fujiwara, K. Hosono, H. Ito, M. Kondo, H. Sakai, M. Tosaki, M. Yasue, S. I. Hayakawa, and R. J. Peterson, Phys. Rev. C **34**, 1530 (1986).
[7] C. Lebo, B. D. Anderson, T. Chittrakarn, A. R. Baldwin, R. Madey, J. W. Watson, and C. C. Foster, Phys. Rev. C **38**, 1099 (1988).
[8] R. J. Peterson, B. L. Clausen, J. J. Kraushaar, H. Nann, W. W. Jacobs, R. A. Lindgren, and M. A. Plum, Phys. Rev. C **33**, 31 (1986).
[9] R. J. Peterson *et al.*, Phys. Rev. C **38**, 1130 (1988).
[10] R. J. Peterson *et al.*, Phys. Rev. C **38**, 2026 (1988).
[11] M. Yasue, H. Sato, T. Hasegawa, J. Takamatsu, T. Terakawa, T. Nakagawa, K. Hatori, and R. J. Peterson, Phys. Rev. C **39**, 2159 (1989).
[12] C. Olmer *et al.*, Phys. Rev. Lett. **43**, 612 (1979).
[13] S. Yen, T. E. Drake, S. Kowalski, C. P. Sargent, and C. Williamson, Phys. Lett. B **289**, 22 (1992).
[14] B. L. Clausen *et al.*, Phys. Rev. Lett. **65**, 547 (1990).
[15] L. Knox, R. A. Lindgren, B. L. Clausen, B. Berman, D. Zubanov, M. Farkhondeh, L. W. Fagg, and M. Manley, Bull. Am. Phys. Soc. **34**, 1812 (1989).
[16] G. S. Blanpied *et al.*, Phys. Rev. C **41**, 1625 (1990).
[17] D. F. Geesaman *et al.*, Phys. Rev. C **30**, 952 (1984).
[18] B. L. Clausen, J. T. Brack, M. R. Braunstein, J. J. Kraushaar, R. A. Loveman, R. J. Peterson, R. A. Ristinen, R. A. Lindgren, and M. A. Plum, Phys. Rev. C **41**, 2246 (1990).
[19] L. Zamick, Phys. Rev. C **29**, 667 (1984).
[20] A. Amusa and R. D. Lawson, Phys. Rev. Lett. **51**, 103 (1983).
[21] J. A. Carr, S. D. Bloom, F. Petrovich, and R. J. Philpott, Phys. Rev. C **45**, 1145 (1992).
[22] F. Petrovich, W. G. Love, A. Picklesimer, G. E. Walker, and E. R. Siciliano, Phys. Lett. **95B**, 166 (1980).
[23] P. Blunden, B. Castel, and H. Toki, Z. Phys. A **312**, 247 (1983).
[24] S. J. Seestrom-Morris, Ph.D. thesis, University of Minnesota, 1981; Los Alamos National Laboratory Report No. LA-8916-T, 1981.
[25] C. L. Morris, L. Atencio, R. L. Boudrie, and S. J. Greene, Los Alamos National Laboratory Progress Report No. LA-11670-PR, 1989, pp. 158–159.
[26] J. J. Kelly, computer code ALLFIT, 1987 (unpublished).
[27] J. Piffaretti, R. Corfu, J.-P. Egger, P. Gretillat, C. Lunke,

E. Schwarz, C. Perrin, and B. M. Preedom, Phys. Lett. **71B**, 324 (1977).
[28] J. P. Albanese, J. Arvieux, J. Bolger, E. Boschitz, C. H. Q. Ingram, J. Jansen, and J. Zichy, Nucl. Phys. **A350**, 301 (1980).
[29] B. Chabloz, R. Corfu, J.-P. Egger, J.-F. Germond, P. Gretillat, C. Lunke, J. Piffaretti, E. Schwarz, C. Perrin, J. E. Bolger, and J. Zichy, Phys. Lett. **81B**, 143 (1979).
[30] R. A. Arndt and L. O. Roper, computer program SAID (Scattering Analysis Interactive Dialin), SM89 solution.
[31] J. A. Carr, F. Petrovich, D. Halderson, and J. Kelly, 1981 version of the computer program ALLWRLD (unpublished).
[32] J. A. Carr, 1981 version of the computer program MSUDWPI (unpublished); adapted from the computer program DWPI of R. A. Eisenstein and G. A. Miller, Comput. Phys. Commun. **11**, 95 (1976).
[33] H. DeVries, C. W. DeJager, and C. DeVries, At. Data Nucl. Data Tables **36**, 495 (1987).
[34] P. D. Kunz, distorted-wave Born approximation code DWUCK4, University of Colorado (unpublished).
[35] R. A. Lindgren, M. Leuschner, B. L. Clausen, R. J. Peterson, M. A. Plum, and F. Petrovich, Can. J. Phys. **65**, 666 (1987).
[36] D. B. Holtkamp, S. J. Seestrom-Morris, D. Dehnhard, H. W. Baer, C. L. Morris, S. J. Greene, C. J. Harvey, D. Kurath, and J. A. Carr, Phys. Rev. C **31**, 957 (1985).
[37] J. A. Carr (unpublished).
[38] J. Cohen, J. Phys. G **13**, 1497 (1987).
[39] F. Petrovich, J. A. Carr, and H. McManus, Annu. Rev. Nucl. Part. Sci. **36**, 29 (1986).